Toward the modelling of surface tension of refrigerant mixture based on linear gradient theory

Zhiheng Wang, Christophe Coquelet, Houriez Céline, Chieko Kondou

Toward the modelling of surface tension of refrigerant mixture based on linear gradient theory

Zhiheng WANG[1,2], Christophe COQUELET[2,3*], Céline HOURIEZ[2], Chieko KONDOU[4]

1. *SJTU-Paris Elite Institute of Technology, Shanghai Jiao Tong University, 800 Dongchuan Road, Minhang District, 200240, Shanghai, China*
2. *MINES Paris, PSL University, CTP – Centre of Thermodynamics of Processes, 35 rue Saint Honoré, 77305 Fontainebleau Cedex, France*
3. *Université de Toulouse, Mines Albi, Centre RAPSODEE UMR CNRS 5302, Campus Jarlard, Albi, France*
4. *Nagasaki University, School of Engineering, Nagasaki, 8528521, Japan*

**Corresponding author:* christophe.coquelet@mines-albi.fr, phone:+33563493141

Abstract

Surface tension is one of the most important thermodynamic properties of the working fluids for the design of heat pumps, refrigerators and air conditioners. The Linear Gradient Theory have been widely used for the prediction of surface tension. Based on this theory and combining with the Peng-Robinson Equation of State, a novel model for surface tension calculation is proposed in this work. In this model, new correlation of pure substance influence parameter (PSIP) with temperature and correlation of binary interaction parameters for influence parameter (BIPc) with temperature and with mass fraction, alongside with the adjustment method for these two parameters are proposed in order to optimize the model. The PSIPs of several common refrigerants and the BIPc of several binary mixtures are adjusted, while the new predictions with these adjusted parameters are done. Results with the adjusted parameters show a great consistency with the experimental data and a great improvement compare to the result obtained with the unadjusted parameters. The adjusted parameters can also be used to predict other mixtures with the same components but with different compositions.

Keywords: Surface Tension; Peng-Robinson Equation of State; Linear Gradient Theory; Influence Parameter; Binary Interaction Parameter

Symbols and Abbreviations

a	Cohesive energy parameter in the PR EoS (J m^3 mol^{-2})
A	Helmholtz free energy (J)
A'	Parameter in the Miqueu et al. equation related to the acentric factor
b	Covolume parameter in the PR EoS (m^3 mol^{-1})
B'	Parameter in the Miqueu et al. equation related to the acentric factor
c	Influence parameter (J m^4 mol^{-2})
E, F	Parameters of Eq. (18)
f_0	Helmholtz free energy density (J m^{-3})
F_{obj}	Objective function
h	Height (m)
k_{ij}	Binary interaction parameter for cohesive parameter a (BIPa)
l_{ij}	Binary interaction parameter for influence parameter c (BIPa)
m	Mass (kg)
n	Mole number or exponent in Eq. (1)
N_{comp}	Number of components
P	Pressure (Pa)
R	Ideal gas constant (J mol^{-1} K^{-1})
T	Temperature (K)
V	Volume (m^3)
v	Molar volume (m^3 mol^{-1})
w	Mass fraction
x	Molar fraction
z	Position in space
AAD	Absolute Average Deviation
ARD	Absolute Relative Deviation
BIAS	Bias
BIPa	Binary interaction parameter for cohesive parameter *a*
BIPc	Binary interaction parameter for influence parameter *c*
CIP	Crossed influence parameter
GWP	Global warming potential
PR EoS	Peng-Robinson Equation of State
PSIP	Pure substance influence parameter

Greek letters

α	α-function
μ	Chemical potential (J mol^{-1})
ρ	Density (kg m^{-3})
σ	Surface tension (N m^{-1})
ϕ	Grand thermodynamic potential (J mol^{-1} m^{-3})
ϕ_B	Negative pressure (J mol^{-1} m^{-3})
ω	Acentric factor

Ω_a, Ω_b	Substance depending factors

Subscript

C	Critical property
cal	Calculated property
comp	Components in the mixture
est	Estimated property using fitting result
exp	Experimental property
i, *j* and *k*	Refrigerant species
L	Largest one in all considered species
ref,REF	Reference property

Superscript

I, II	Number of bulk phase
0	Pure substance bulk phase property
*	Ideal gas state property
res	Residual term

1 Introduction

Fluorinated components are wildly used as the refrigerants in the industries. As preventing global warming and ozone layer depletion has become one of the most concerning issues for environmental protection, developing refrigerant with lower global warming potential (GWP) has been a major trend of research in the recent years. The knowledge of the thermodynamic properties and the phase diagram of these refrigerants is essential in the industrial application. Surface tension, as a fundamental thermodynamic property, which can influence the heat transfer, flow, and the phase-change character, is required for the design of the refrigerators[1, 2].

When developing new refrigerant compounds, the number of candidates can be very considerable, which makes it difficult to obtain detailed experimental data for all the possible candidates. On the contrary, using predictive models can reduce greatly the cost and time. In the previous studies, several methods for predicting the surface tension have been proposed, including the parachor method [3-6] and its derivatives, the corresponding-states principle [7-9], the Monte Carlo simulation [10, 11], the perturbation theory [12, 13], and gradient theory [14-23] to mention only a few. Besides, Zuo and Stenby developed the Linear Gradient Theory (LGT) [24] based on the gradient theory, simplifying the density gradient in a mixture as linear, thus reduced the calculation time without losing accuracy.

In this work, a new model for calculating the surface tension based on the LGT is proposed for both pure substance and binary mixtures. Several pure refrigerants' surface tensions are calculated with this model and compared with the experimental data in the previous studies. Then the influence parameters for these substances are adjusted in order to better fit the reality. After that, the surface tensions for several binary mixtures are calculated with model and with the previously adjusted influence parameters. Besides, by comparing the experimental data with the simulations for these binary mixtures, a new correlation for the binary interaction coefficient based on temperature and composition is established so as to optimize the model.

2 Model

2.1 Equation of State

In this work, the Peng-Robinson Equation of State (PR EoS) [25] is applied (Eq. (1)) to represent the thermodynamic properties of the bulk phase of the fluids.

$$P = \frac{RT}{v-b} - \frac{a(T)}{v^2+2bv-b^2} \tag{1}$$

where P is the pressure, T is the temperature, R is the ideal gas constant, v the molar volume, and

$$a(T) = a_c\alpha(T) \tag{2}$$

$$a_c = \Omega_a \frac{R^2 T_c^2}{P_c} \tag{3}$$

$$\alpha(T) = \left[1 + m\left(1 - T_R^{1/2}\right)\right]^2 \tag{4}$$

$$m = 0.374640 + 1.542260\omega - 0.26992\omega^2 \tag{5}$$

$$b = \Omega_b \frac{RT_c}{P_c} \tag{6}$$

with T_c and P_c the critical temperature and pressure, ω the acentric factor, $T_R = \frac{T}{T_c}$, $\Omega_a = 0.457240$, and $\Omega_b = 0.07780$. It is also worth mentioning that in this research, for the mixtures, a mixing rule of van der Waals, also known as the classical mixing rule[26], is applied, which is represented with the following equations.

For the mixture, we have considered the classical mixing rule (Eq. (7)).

$$a = \sum_i \sum_j x_i x_j a_{ij} \text{ and } b = \sum_i x_i b_i \tag{7}$$

with $a_{ij} = \sqrt{a_i a_j}(1 - k_{ij})$, x_i and x_j are the mole fraction of the component i and j, and a_i, b_i are respectively the cohesive energy parameter a and the covolume parameter b in the PR EoS for component i, and k_{ij} is the binary interaction parameter (BIPa) for the cohesive parameter a. In this research, all the BIPa used are calculated with the model of E-PPR78 proposed by Qian et al.[27] based on the group contribution method.

2.2 Linear Gradient Theory

The Gradient Theory (GT) has been thoroughly investigated in the previous studies [14-23, 28], so here, only the framework and essential equations of the Linear Gradient theory (LGT) are presented. According to GT, before the calculation of the surface tension, a series of equations should be solved so as to acquire the density profile in the mixture. In order to eliminate this time-consuming process, without significantly losing the accuracy[29], an assumption is introduced where the density of each component in the mixture between bulk phase is assumed to be linearly distributed. In this research, the molar density (noted as ρ) is used. For a planar interface with a height h, the molar density of component i among the N_{comp} (number of components) components at position z is given by Eq. (8).

$$\frac{d\rho_i(z)}{dz} = D_i \qquad i = 1, 2, \dots, N_{comp} \tag{8}$$

where D_i is a constant for each component i, and we also have to consider Eq. (9).

$$D_i = \frac{\Delta\rho_i}{h} = \frac{\rho_i^{\mathrm{II}} - \rho_i^{\mathrm{I}}}{h} \tag{9}$$

where ρ_i^{I} and ρ_i^{II} denote the molar density of the bulk phase I and II, while $\Delta\rho_i$ is well the

difference between these two molar densities. Similar to the GT, the surface tension is calculated with Eq. (10).

$$\sigma = \int_{\rho_{\mathrm{ref}}^{\mathrm{I}}}^{\rho_{\mathrm{ref}}^{\mathrm{II}}} \sqrt{2c(\phi(\rho) - \phi_B)}\mathrm{d}\rho_{\mathrm{ref}} \tag{10}$$

where c is the influence parameter, whose calculation method will be presented in the section 2.3, $\phi(\rho)$ is the grand thermodynamic potential, ϕ_B is the negative pressure ($-P_B$). The subscript ref represents that a reference density is used in this calculation. The selection of this reference molar density will also be discussed in the section 2.4.

According to its definition, the grand thermodynamic potential (Eq. (11)) is determined via the Helmholtz free energy density of the mixture $f_0(\rho)$ and the chemical potential of bulk phase μ_i^0 for each component i.

$$\phi(\rho) = f_0(\rho) - \sum_i \rho_i \mu_i^0 \tag{11}$$

In this equation, the $f_0(\rho)$ (Eq. (12)) can be obtained from the Helmholtz free energy A, which can be divided into a term A^* representing the contribution of the pure substances in their ideal gas state and a residual term A^{res}.

$$f_0(\rho) = \frac{A(T,V,\vec{n})}{V} = \frac{A^*(T,V,\vec{n})}{V} + \frac{A^{\mathrm{res}}(T,V,\vec{n})}{V} \tag{12}$$

where V is the total volume of the mixture and $\vec{n}$ is a vector containing the amount of substance for each component i. Then the $f_0(\rho)$ can be calculated by Eq. (13).

$$f_0(\rho) = \sum_i \rho_i \mu_i^*(T, P^{REF}) + RT\sum_i \rho_i \ln\left(\frac{\rho_i RT}{P^{REF}}\right) - \rho RT - \rho RT\ln\left(\frac{P}{\rho RT}\right)$$
$$-\rho RT\ln(1-\rho b) + \frac{\rho a}{2\sqrt{2}b}\ln\left(\frac{1+(1-\sqrt{2})\rho b}{1+(1+\sqrt{2})\rho b}\right) \tag{13}$$

The chemical potential μ_i^0 (Eq. (14)) can be obtained from the derivative of the Helmholtz energy with respect to the amount of substance for each component, or, the derivative of the Helmholtz energy density with respect to the molar density. Similarly, due to the presence of Helmholtz free energy, can also be divided into a term representing the contribution of components in an ideal gas state and a residual term.

$$\mu_i^0 = \mu_i^*(T, P^{REF}) + RT\ln\left(\frac{\rho_i RT}{P^{REF}}\right) - RT\ln\left(\frac{P}{\rho_i^0 RT}\right) - \frac{\sum_j \rho_j a_{ij}}{\sqrt{2}\rho b}\ln\left(\frac{1+(1-\sqrt{2})\rho b}{1+(1+\sqrt{2})\rho b}\right) + \frac{\rho RT b_i}{(1-\rho b)}$$
$$+\frac{ab_i}{2\sqrt{2}b^2}\ln\left(\frac{1+(1-\sqrt{2})\rho b}{1+(1+\sqrt{2})\rho b}\right) - RT\ln(1-\rho b) - \frac{\rho b_i a}{b(1+(1-\sqrt{2})\rho b)(1+(1+\sqrt{2})\rho b)} \tag{14}$$

In this equation, all the superscripts 0 denote the bulk phase, while the a_{ij} is the same a_{ij} in the Eq. (7). In fact, the first two terms in both $f_0(\rho)$ and μ_i^0 which represent the ideal gas state term will cancel each other out in the calculation of $\phi(\rho)$ (c.f. Eq. (11)), so in the real calculations,

there is no need for searching for a reference pressure, only calculating the residual terms of $f_0(\rho)$ and μ_i^0 will be enough.

2.3 Influence parameters

For Eq. (10), the calculation method of the influence parameter c should correspond to the choice of the reference molar density ρ_{ref}. Nonetheless, no matter which reference is chosen, the crossed influence parameters c_{ij} (CIPs) are essential for further calculation. It can be obtained from the pure substance influence parameter c_i (PSIP) (Eq. (15)) which is firstly proposed by Carey[30].

$$c_{ij} = \sqrt{c_i c_j}(1 - l_{ij}) \tag{15}$$

where l_{ij} is binary interaction parameter of influence parameter c (BIPc), if $l_{ij} = 0$, the CIPs are the geometry mean of the PISP, and in analogy with the BIPa k_{ij} (Eq. (16)).

$$l_{ij} = l_{ji} \text{ and } l_{ii} = 0, \ \forall i, j = 1, 2, \dots, N_{comp} \tag{16}$$

Besides, combining the symmetry of Eq. (15) with Eq. (16), we obtained Eq. (17).

$$c_{ii} = c_i \text{ and } c_{ij} = c_{ji}, \ \forall i, j = 1, 2, \dots, N_{comp} \tag{17}$$

As for the PISPs, being inspired by the work of Zuo and Stendy[28], this work has used Eq. (18).

$$\frac{c_i}{a_i b_i^{2/3}} = E_i(1 + T_r)^{F_i} \tag{18}$$

where a_i, b_i are respectively the constant a and b in the PR EoS for component i, E_i and F_i are two coefficients depending on the substance, to be more specific, depending on the acentric factor with the Eq. (19).

$$E_i = \frac{1}{e_1 + \omega_i e_2} \text{ and } F_i = \frac{1}{e_3 + \omega_i e_4} \tag{19}$$

where e_1, e_2, e_3 and e_4 are four constants which will be determined with the method introduced in section 2.5. Our choice concerning the equations of E_i and F_i is in consistance with equations selected by Miqueu et al. 2003 [15], for the prediction of influence parameter c. In fact, the polynomial equations proposed by Zuo and Stenby [28] can lead to important deviations if the model is applied in predictive way for molecules when their acentric factor are not in the range of acentric factors of molecules considered in the fitting procedures.

2.4 Reference molar density

In general, the molar density of either the mixture or one of the components can be chosen as the reference, so in the following parts, two approaches of choosing the reference and its corresponding method for calculating the influence parameter will be presented.

2.4.1 Density gradient approach

The first approach consists in choosing the component with the maximal difference between the molar density of the two phases in equilibrium in order to have a maximal coverage in the integral (Eq. (20).

$$\rho_{\mathrm{ref}} = \rho_L \text{ with } \Delta\rho_L = \max(\Delta\rho_i) \quad i = 1, 2, \dots, N_{comp} \tag{20}$$

The subscript L denotes that this is the component with the "Largest" difference of molar density. For this type of reference molar density, the influence parameter should be determined with the difference of the molar density (Eq. (21)).

$$c = \sum_i \sum_j c_{ij} \left(\frac{\Delta\rho_i}{\Delta\rho_L}\right)\left(\frac{\Delta\rho_j}{\Delta\rho_L}\right) \tag{21}$$

2.4.2 Mole fraction approach

The molar density of the mixture can be also chosen as the reference (Eq. (22)).

$$\rho_{\mathrm{ref}} = \rho \text{ with } \rho = \sum_i \rho_i \text{ and } \rho_i = x_i\rho \tag{22}$$

where the x_i is the mole fraction of component i in the liquid phase. For this type of reference, the influence parameter is determined with the mole fractions by Eq. (23).:

$$c = \sum_i \sum_j x_i x_j c_{ij} \tag{23}$$

It is worth mentioning that if the studied fluid is well a pure substance ($N_c = 1$), for both approaches, we shall have $c = c_1$, since $\Delta\rho_i = \Delta\rho_L$ or $x_1 = 1$. This property is the basis of the adjustment of the PSIP, which will be discussed in the next section.

2.5 Pure substance influence parameter adjustment

As it is discussed in the previous section, for a pure substance, $c = c_1$, besides, since c is independent to a variable of molar density inside the integral, Eq. (10) can well be rewritten as Eq. (24).

$$\sigma = \sqrt{c_1} \int_{\rho_{\mathrm{ref}}^{\mathrm{I}}}^{\rho_{\mathrm{ref}}^{\mathrm{II}}} \sqrt{2(\phi(\rho) - \phi_B)}\mathrm{d}\rho_{\mathrm{ref}} \tag{24}$$

if we note $\sigma_{cal} = \int_{\rho_{\mathrm{ref}}^{\mathrm{I}}}^{\rho_{\mathrm{ref}}^{\mathrm{II}}} \sqrt{2(\phi(\rho) - \phi_B)}\mathrm{d}\rho_{\mathrm{ref}}$, then Eq. (24) becomes Eq. (25).

$$c_1 = \frac{\sigma^2}{\sigma_{cal}^2} \tag{25}$$

By injecting this equation into Eq. (18), we have Eq. (26).

$$E_1(1+T_r)^{F_1} = \frac{c_1}{a_1 b_1^{2/3}} = \frac{\sigma^2}{\sigma_{cal}^2}\frac{1}{a_1 b_1^{2/3}} \tag{26}$$

Recalling here that a_1 is also depending on the temperature, Eq. (26) can be written as Eq. (27).

$$E_1\left(1+\frac{T}{T_c}\right)^{F_1} = \frac{\sigma^2(T)}{\sigma_{cal}^2(T)}\frac{1}{a_1(T) b_1^{2/3}} \stackrel{\text{def}}{=} D \tag{27}$$

On the right side of this equation, by introducing a group of N experimental surface tension data with different temperatures, noted as $\{\sigma_{\text{exp},k}(T),\ k=1,2,\dots,N_1\}$, we can calculate the experimental D, noted as $\left\{D_{\text{exp},k}(T) = \frac{\sigma_{\text{exp},k}^2(T)}{\sigma_{cal}^2(T)}\frac{1}{a_1(T) b_1^{2/3}},\ k=1,2,\dots,N_1\right\}$. On the left side, the set of estimated D, noted as $\left\{D_{\text{est},k}(T) = E_{1,\text{est}}\left(1+\frac{T}{T_c}\right)^{F_{1,\text{est}}},\ k=1,2,\dots,N_1\right\}$ is calculated with the estimated $E_{1,\text{est}}$ and $F_{1,\text{est}}$. Now, an objective function is defined by Eq. (28).

$$F_{obj,1}(E_{1,\text{est}}, F_{1,\text{est}}) = \sum_{k=1}^{N_1}\left(\frac{D_{\text{est},k}(T) - D_{\text{exp},k}(T)}{D_{\text{exp},k}(T)}\right)^2 \tag{28}$$

The adjustment of the pair $(E_{1,\text{est}}, F_{1,\text{est}})$ is in fact the search for a such pair that minimizes the objective function $F_{obj,1}$, and the adjusted influence parameter for this substance can be calculated with the pair $(E_{1,\text{est}}, F_{1,\text{est}})$ and with Eq. (18). In order to have a more comprehensive estimation of PSIP for other substance, the constants e_1, e_2, e_3 and e_4 remind to be determined. After repeating the process of searching for the pair $(E_{1,\text{est}}, F_{1,\text{est}})$ for a sufficient amount of substance, we can move to the adjustment of e_1, e_2, e_3 and e_4. Similarly, the dataset of estimated $E_{i,\text{est}}$ and $F_{i,\text{est}}$ of N_2 substance is noted as $\{E_{i,\text{est}}(\omega_i),\ F_{i,\text{est}}(\omega_i),\ i=1,2,\dots,N_2\}$, while that calculated with e_1, e_2, e_3 and e_4 is noted as $\left\{E_{i,\text{cal}}(\omega_i) = \frac{1}{e_1+\omega_i e_2},\ F_{i,\text{cal}}(\omega_i) = \frac{1}{e_3+\omega_i e_4},\ i=1,2,\dots,N_2\right\}$. We can define 2 other objective functions similar to $F_{obj,1}$ (Eqs.(29-30)).

$$F_{obj,2}(e_1, e_2) = \sum_{i=1}^{N_2}\left(\frac{E_{i,\text{est}}(\omega_i) - E_{i,\text{cal}}(\omega_i)}{E_{i,\text{est}}(\omega_i)}\right)^2 \tag{29}$$

$$F_{obj,3}(e_3, e_4) = \sum_{i=1}^{N_2}\left(\frac{F_{i,\text{est}}(\omega_i) - F_{i,\text{cal}}(\omega_i)}{F_{i,\text{est}}(\omega_i)}\right)^2 \tag{30}$$

Similarly, the adjusted group of constants e_1, e_2, e_3 and e_4 is in fact a such group that minimize $F_{obj,2}$ and $F_{obj,3}$. In the end, with all the coefficients and constants adjusted, given with the temperature and the acentric factor of a studied fluid, its PSIP can be calculated with Eq. (19) then with Eq. (18).

2.6 Binary interaction parameter adjustment

Unlike the PSIP, the BIP only occurs when the studied fluid is well a mixture. Since the determination method of BIPa has already been mentioned in the previous section, here in this section, only the calculation and adjustment method for the BIPc l_{ij} will be discussed. Besides, in this work, we mainly focus on the binary mixtures ($N_c = 2$); thus, according to Eq. (16), only l_{12} need to be determined and adjusted.

As can be found in the experimental data on the surface tension of the binary mixtures in the previous research, l_{12} for two substances depend on both the temperature and the composition of the mixture. Since in the prior works, mass fractions are usually used to represent the composition of the mixture, we also use in this work the mass fraction w_i of the component i as the measurement for the composition. In addition, by convention, when $w_1 = 0$ or 1, the mixture is well a pure substance, so we define $l_{12}(w_1 = 0 \text{ or } 1) = 0$. As a result, we use Eq. (31) for the calculation of l_{12} with T and w_1:

$$l_{12}(T, w_1) = w_1(1 - w_1)(A(T) + B(T)(w_1 - w_2) + C(T)(w_1 - w_2)^2) \tag{31}$$

where $A(T)$, $B(T)$ and $C(T)$ are three coefficients which depend only on the temperature (Eq. (32)).

$$A(T) = A_1 \cdot T + \frac{A_2}{T - A_3} \text{ and } B(T) = B_1 \cdot T + \frac{B_2}{T - B_3} \text{ and } C(T) = \frac{C_1}{(T - C_3)^3} - \frac{C_2}{(T - C_3)^4} + C_4 \tag{32}$$

where A_1, A_2, A_3, B_1, B_2, B_3, C_1, C_2, C_3 and C_4 are ten temperature-independent parameters that need to be determined for one pair of substance. One can easily found that with this correlation, $l_{12}(T, 0) = l_{12}(T, 1) = 0$, while we also have $w_1 + w_2 = 1$, since this is well a binary mixture.

The first step of adjustment l_{12} consists in finding the value of the three temperature-dependent coefficients under constant temperature with the help of different mass fractions. However, before moving into the detailed adjustment process, l_{12} need to be calculated with the experimental data. Similar to the adjustment of PSIP, we start with Eq. (10) by extracting the influence parameter, by using the same notation as the adjustment of PSIP, we consider Eq. (33).

$$c = \frac{\sigma^2}{\sigma_{cal}^2} \tag{33}$$

Only this time, the influence parameter c is no longer equal to the PSIP of one component but a sum of a few terms. As it is discussed in section 2.3, two different approaches can be used to calculate c, however, in this section, only the first density gradient approach for choosing the reference density is used to demonstrate the adjustment of l_{12}. We can derive from Eqs. (15 and 21) that for a binary mixture (Eq. (34)).

$$c = c_1 \left(\frac{\Delta\rho_1}{\Delta\rho_L}\right)^2 + c_2 \left(\frac{\Delta\rho_2}{\Delta\rho_L}\right)^2 + \left(\frac{\Delta\rho_1}{\Delta\rho_L}\right)\left(\frac{\Delta\rho_2}{\Delta\rho_L}\right)\sqrt{c_1 c_2}(1 - l_{12}) \tag{34}$$

Then combining Eqs. (32 and 34), we obtain Eq. (35).

$$l_{12} = 1 - \frac{\frac{\sigma^2}{\sigma_{cal}^2} - c_1\left(\frac{\Delta\rho_1}{\Delta\rho_L}\right)^2 - c_2\left(\frac{\Delta\rho_2}{\Delta\rho_L}\right)^2}{\left(\frac{\Delta\rho_1}{\Delta\rho_L}\right)\left(\frac{\Delta\rho_2}{\Delta\rho_L}\right)\sqrt{c_1 c_2}} \quad (35)$$

Similarly, by introducing the experimental data of surface tension, we can calculate the dataset of $l_{12,\mathrm{exp}}$ with N_3 different mass fractions under a given temperature. Then with the correlation defined in Eq. (35), and with an estimated group $(A(T), B(T), C(T))$, we can calculate the estimate l_{12} with the same temperature, noted as $l_{12,\mathrm{est}}$. We can also define another objective function (Eq. (36)).

$$F_{obj,4}(A(T), B(T), C(T)) = \sum_{i=1}^{N_3}\left(\frac{l_{12,\mathrm{exp}} - l_{12,\mathrm{est}}}{l_{12,\mathrm{exp}}}\right)^2 \quad (36)$$

In this way, the adjustment of the group $\left(A_{\mathrm{est}}(T), B_{\mathrm{est}}(T), C_{\mathrm{est}}(T)\right)$ consists of finding such a group that minimizes the objective function $F_{obj,4}$.

After calibrating the group $(A(T), B(T), C(T))$ with different temperatures, we can move on to the determination of the nine constants to establish the expressions of $(A(T), B(T), C(T))$. Similarly, we can calculate the group $\left(A_{\mathrm{cal}}(T_i), B_{\mathrm{cal}}(T_i), C_{\mathrm{cal}}(T_i)\right)$ with the estimated value of the nine constants and compare it with the group $\left(A_{\mathrm{est}}(T_i), B_{\mathrm{est}}(T_i), C_{\mathrm{est}}(T_i)\right)$ obtained in the previous step by using the objective functions defined by Eqs. (37-39).

$$F_{obj,5}(A_1, A_2, A_3) = \sum_{i=1}^{N_4}\left(\frac{A_{\mathrm{cal}}(T_i) - A_{\mathrm{est}}(T_i)}{A_{\mathrm{est}}(T_i)}\right)^2 \quad (37)$$

$$F_{obj,6}(B_1, B_2, B_3) = \sum_{i=1}^{N_4}\left(\frac{B_{\mathrm{cal}}(T_i) - B_{\mathrm{est}}(T_i)}{B_{\mathrm{est}}(T_i)}\right)^2 \quad (38)$$

$$F_{obj,7}(C_1, C_2, C_3, C_4) = \sum_{i=1}^{N_4}\left(\frac{C_{\mathrm{cal}}(T_i) - C_{\mathrm{est}}(T_i)}{C_{\mathrm{est}}(T_i)}\right)^2 \quad (39)$$

Then this last step consists in searching for a group of these nine constants that minimize these three objective functions.

3 Results and discussion

As the method is based on the evaluation of the density gradient, we have checked the predicted densities deviations between PR EoS and REFPROP for the pure component and the mixtures. The results are presented in the Supplementary File. As we can see, the PR EoS under predicts the liquid densities. We can consider that it is not a problem as the parameters of influence parameter or the BIPc are adjusted on experimental data. The problem concerning surface tension calculation happens only close to the pure component and mixture critical point.

3.1 Prediction of the surface tension before adjustment

The very first application of the model focuses on the prediction of the surface tension for a

pure substance. Due to a lack of the prior adjustment of PSIP for the model, the expressions for the PSIP presented in the work of Miqueu et al., which is proven suitable for the gradient theory combining with the PR EoS model, is used in this part. These expressions are given by[16]:

$$\frac{c_i}{a_i b_i^{2/3}} = A'_i t_i + B'_i \tag{40}$$

where $t_i = 1 - T/T_c$ the reduced temperature, while A_i and B_i are two coefficients related to the acentric factor as:

$$A'_i = \frac{-10^{-16}}{1.2326+1.3757\omega_i}$$

$$B'_i = \frac{-10^{-16}}{0.9051+1.5410\omega_i} \tag{41}$$

The surface tensions of several common refrigerants are calculated with the model. The results are then compared with the experimental data in the prior works. Table 1 shows relative information of the tested refrigerants.

The results are shown in Fig. S1 in supplementary file. In general, even without calibrating the influence parameter, the calculated results still show a high consistency with the experimental data, which shows the validity of the model. Nonetheless, some small differences (e.g., Fig. S1 (a), (h) at a low temperature and Fig. S1 (i)) can still be observed between the prediction and the experiment, which has induced a necessity of the adjustment.

Table 1: Tested refrigerants, their critical temperatures, critical pressures, acentric factors, reference number for the thermodynamic properties and for the experimental data

Refrigerant	T_C /K	P_C MPa	ω	Properties' reference	Data's reference
R32	351.26	5.782	0.2769	REFPROP	[32]
R125	339.17	3.6177	0.3052	REFPROP	[33]
R134a	374.21	4.0593	0.32684	REFPROP	[33]
R152a	386.41	4.5168	0.27521	REFPROP	[33]
R1123	331.73	4.5426	0.261	REFPROP	[32]
R1233zd(E)	438.75	3.573	0.3050	[34]	[34]
R1234yf	367.85	3.382	0.280	[35]	[35, 36]
R1234ze(E)	382.51	3.6349	0.313	REFPROP	[37]
R1234ze(Z)	423.27	3.533	0.3274	[34]	[34]
R1243zf	376.93	3.517	0.2605	[34]	[34]

3.2 Adjustment of PSIP

In order to better calibrate the related coefficient and constants for calculating influence parameter, more refrigerants are introduced in this part. Table 2 presents the relative information regarding all the refrigerants used in this part. It is worth mentioning that for some of the substances, not all the data from the reference are used in the adjustment process. The unused data are mainly concentrated on the data with the temperature near the critical points, and the calculated results with these unused data show some enormous differences with the experimental data. This is mainly caused by the default of the PR EoS near the critical points, where certain hypotheses are no longer valid. Thus, the densities of the two phases at equilibrium calculated by using this equation of state, which are essential for the later calculation of the surface tension, are not corresponding to the experimental data.

The results of the adjustments of the coefficients E_i and F_i, which are used to calculate the PSIP with Eq. (18) for these refrigerants, are shown in Table 3. Besides, in order to evaluate the quality of the adjustment in all the results of adjustments, the Average Relative Deviation (ARD) or the Average Absolute Deviation (AAD) and the bias (BIAS) of the adjustment are calculated with the Eq. (42), where $X_{i,\mathrm{exp}}$ and $X_{i,\mathrm{cal}}$ denote respectively parameter X obtained from experiments and the adjusted parameter X.

$$ARD = \frac{100}{N}\sum_{i=1}^{N}\left|\frac{X_{i,\mathrm{exp}}-X_{i,\mathrm{cal}}}{X_{i,\mathrm{exp}}}\right| \tag{42a}$$

$$AAD = \frac{100}{N}\sum_{i=1}^{N}\left|X_{i,\mathrm{exp}}-X_{i,\mathrm{cal}}\right| \tag{42b}$$

$$BIAS = \frac{100}{N}\sum_{i=1}^{N}\frac{X_{i,\mathrm{exp}}-X_{i,\mathrm{cal}}}{X_{i,\mathrm{exp}}} \tag{42c}$$

Table 2: Used refrigerants for the adjustment of PSIP reference number for the thermodynamic properties, and the experimental data.

Refrigerant	Properties' reference	Data's reference	Amount of data used
R32	[38]	[39]	5
R125	[40]	[33]	11
R152a	[41]	[33]	12
R134a	[42]	[33]	14
R143a	[43]	[33]	10
R1234ze(Z)	[44]	[34]	13
R1243zf	[45]	[34]	11

Table 3: Used refrigerants for the adjustment of PSIP, acentric factors, adjusted E_is and F_is, with ARD and BIAS for the adjustments

Refrigerant	ω	E_i ($\times 10^{-17}$)	F_i	ARD (%)	BIAS (%)
R32	0.2769	3.440	-0.3580	1.2	-0.019
R125	0.3052	3.396	-0.3653	0.93	-0.011
R152a	0.27521	2.957	-0.4776	0.61	-0.0066
R134a	0.32684	3.315	-0.3444	1.3	-0.029
R143a	0.2615	3.378	-0.4304	0.38	-0.0017
R1234ze(Z)	0.327	3.100	-0.4767	1.8	-0.40
R1243zf	0.2604	3.438	-0.4166	1.6	-0.044

With these adjusted E_is and F_is, we can then determine the four constants e_1, e_2, e_3 and e_4 (c.f. Eq. (19)) in order to summarize a general expression that relate these two coefficients with the acentric factor. The results are shown in the Table 4.

Table 4: Adjusted results for e_1, e_2, e_3 and e_4 with ARD and BIAS.

e_1 ($\times 10^{16}$)	e_2 ($\times 10^{16}$)	ARD /%	BIAS /%
2.658	1.378	4.81%	0.559%
e_3	e_4	ARD /%	BIAS /%
-1.462	-3.623	10.4%	0.654%

By injecting these constants into Eq. (19), we now have the expression for any E_i and F_i as a function of acentric factor and given by Eq. (43).

$$E_i = \frac{10^{-16}}{2.658+1.378\omega_i} \text{ and } F_i = -\frac{1}{1.462+3.623\omega_i} \quad (43)$$

3.3 Adjustment of BIPc

All the calculated results were also compared with calculations done by a modified Mulero et al.[46] correlations adapted for mixtures. More details concerning the development of the method are given in the Supplementary File.

3.3.1 R32+R134a binary system

A binary mixture of R32 (Component 1) and R134a (Component 2) is used as a first example to demonstrate the adjustment of BIPc. The thermodynamic properties of these two refrigerants can be found in Table 2, while the experimental data presented in the work of Duan et al.[47] are used for the adjustment. In addition, the already adjusted expression for calculating PSIP (Eq. (43))

is used in this part.

Theoretically, the first step is to use the data with constant temperature but different compositions to calibrate the three temperature-dependent coefficients. However, in most of the prior works, the experiments are done with constant composition and by changing the temperature, and it is difficult to find the data with exactly the same temperature but different composition (e.g., the data in the work of Duan et al.[47]). Thus, before the adjustment, a fitting process needs to be done to reconstruct the experimental dataset and obtain a continuous group of data with respect to the temperature.

In this work, for the experimental data in the work of Duan et al.[47], Eq.(44) is used to do the fitting for the BIPc calculated from the experimental data (for a fixed w_1).

$$l_{12,\mathrm{fit}}(T) = l_a T + \frac{l_b}{T - l_c} \tag{44}$$

where l_a, l_b and l_c are three constants to be determined concerning w_1. We can define a similar objective function given by Eq. (45).

$$F_{obj,8}(l_a, l_b, l_c) = \sum_{i=1}^{N_5} \left(\frac{l_{12,\mathrm{fit}}(T_i) - l_{12,\mathrm{exp}}(T_i)}{l_{12,\mathrm{exp}}(T_i)} \right)^2 \tag{45}$$

and search for the group (l_a, l_b, l_c) that minimizes this objective function.

Table 5: Values of Eq. (44)'s parameters l_a, l_b and l_c for the four studied w_1 for the R32 (1) + R134a (2) binary system.

w_1	23.79%	40.17%	62.35%	76.28%
l_a ($\times 10^{-10}$K^{-1})	1.000	1.000	1.000	1.000
l_b ($\times 10^{1}$)	9.238	7.724	7.491	7.537
l_c ($\times 10^{2}$K)	3.555	3.414	3.364	3.377
ARD (%)	3.1	2.5	6.2	7.1
BIAS (%)	0.14	-0.090	-0.57	-0.67

Table 5 shows the results for the adjusted l_a, l_b and l_c for the four studied mass fractions in the work of Duan et al., while the comparison between the fitting data and original data calculated from experimental data is shown in Fig. 1.

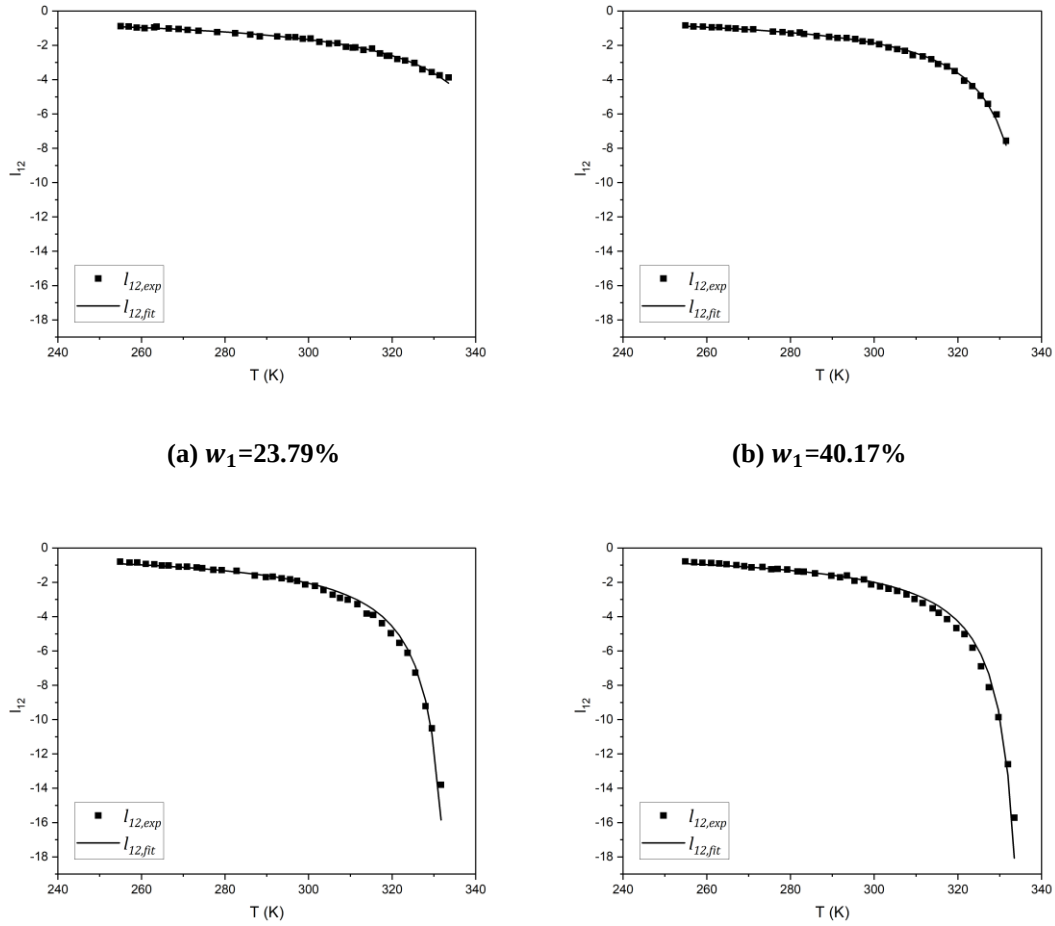

(a) w_1=23.79% **(b) w_1=40.17%**

(c) w_1=62.35% **(d) w_1=76.28%**

Figure 1: $l_{12,\mathrm{fit}}$ compared with $l_{12,\mathrm{exp}}$ for the four studied w_1 for the R32 (1) + R134a (2) binary system.

This reconstructed and enlarged dataset is then used to calibrate the 3 temperature-dependent coefficients. The adjusted coefficients are shown in Table 6, while the adjusted l_{12} with respect to w_1 under different temperatures is shown in Fig. 2.

Table 6: Values of Eq. (31)'s parameters A, B and C for different temperatures for the R32 + R134a binary system.

T /K	*A*	*B*	*C*	ARD /%	BIAS /%
260	-3.715	-0.2206	-6.890	0.65	-0.0046
270	-4.266	-0.3746	-7.631	0.52	-0.0030
280	-5.008	-0.6231	-8.539	0.37	-0.0015
290	-6.061	-1.050	-9.667	0.21	-0.00048
300	-7.672	-1.856	-11.08	0.059	-0.000032
310	-10.44	-3.603	-12.80	0.011	0.000013
320	-16.25	-8.463	-14.52	0.505	-0.0030

330	-35.55	-32.44	-15.25	4.7	-0.29
335	-76.96	-118.9	-53.37	18	-5.9

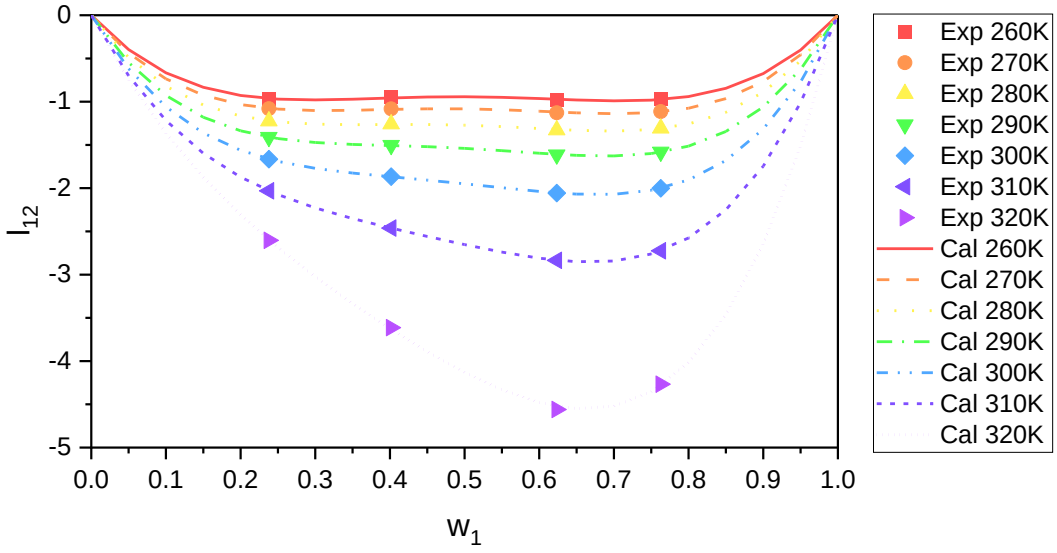

Figure 2: l_{12} obtained from experiments (Exp) and adjusted l_{12} (Cal) vs w_1 under different temperatures for the R32 (1) + R134a (2) binary system.

Table 7: Values of Eq. (32)'s temperature-independent parameters for the BIPc for the R32 (1) + R134a (2) binary system.

Constant	Value	Constant	Value	Constant	Value
A_1 ($\times 10^{-3}$)	1.171	B_1 ($\times 10^{-3}$)	6.657	C_1 ($\times 10^{3}$)	-2.537
A_2 ($\times 10^{2}$)	3.193	B_2 ($\times 10^{2}$)	1.358	C_2 ($\times 10^{4}$)	2.946
A_3 ($\times 10^{2}$)	3.389	B_3 ($\times 10^{2}$)	3.359	C_3 ($\times 10^{2}$)	3.391
				C_4 ($\times 1$)	-7.184

Table 8: ARD and BIAS of fitting parameters *A*, *B* and *C* with the ten adjusted constants for the R32 + R134a binary system.

	A	*B*	*C*
ARD /%	0.63	16	10
BIAS /%	-0.0062	-4.0	-1.7

By using these data relating temperature-dependent coefficients with the temperatures, the ten temperature-independent constants A_1, A_2, A_3, B_1, B_2, B_3, C_1, C_2, C_3 and C_4 can be determined and the relations in Eq. (32) can be established. Table 7 presents the adjusted temperature-independent constants, while the Table 8 shows the ARD and BIAS of the fitting for

$\left(A(T), B(T), C(T)\right)$ using theses ten adjusted constants. Meanwhile, Fig. S2 presents a comparison between temperature-dependent coefficients for BIPc calculated from the experimental data and from the estimated group of ten temperature-independent constants.

Table 9: ARD and BIAS for the predictions compared to the experimental data for the four studied w_1. for the R32 (1) + R134a (2) binary system.

w_1	23.79%	40.17%	62.35%	76.28%
ARD /%	2.1	0.99	2.2	2.4
BIAS /%	1.4	0.59	-1.4	-1.2

With all these coefficient and constants adjusted, a new prediction of the surface tension can be well acquired. The results of the predictions, compared with the original experimental data and with calculated surface tensions with unadjusted BIPc ($l_{12} = 0$) are shown in the Fig. 3, while the ARDs for all 4 studied w_1 are presented in the Table 9.

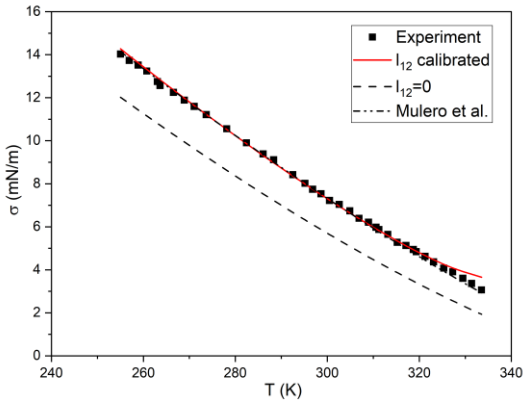

(a) w_1=23.79%

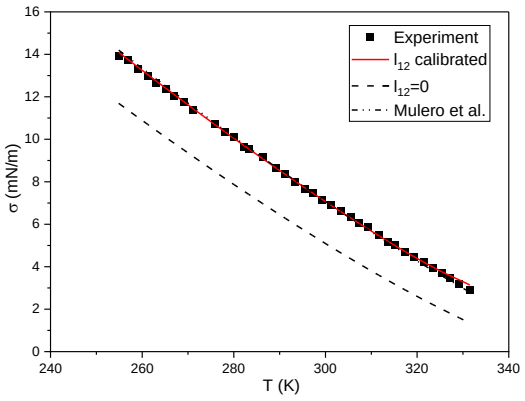

(b) w_1=40.17%

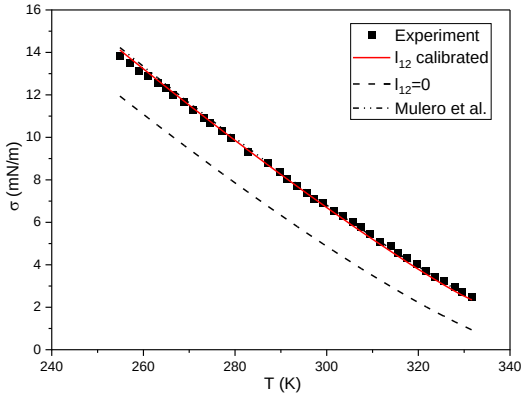

(c) w_1=62.35%

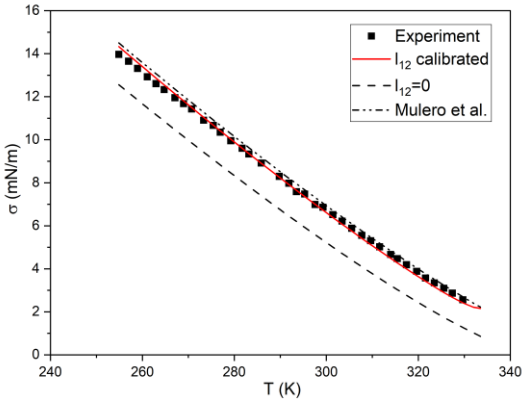

(d) w_1=76.28%

Figure 3: Surface tensions predicted by the model with the adjusted l_{12} compared with experimental data, with surface tensions calculated with unadjusted l_{12} ($l_{12} = 0$) and with method proposed by Mulero et al. (supplementary file) for the R32 (1) + R134a (2) binary system.

From the results presented above, we can see clearly the prediction with adjusted l_{12} has a good consistency with the experimental data (with an ARD around 2%). However, compared to the prediction with $l_{12} = 0$ (which means that the CIP is just the geometric mean of the PSIP), prediction with adjusted l_{12} are much closer to the experimental data. It demonstrates the effectiveness of the adjustment and of the model.

3.3.2 R32+R125 and R125+R152a

Besides, the same adjusted process is implemented with other binary mixtures, including mixtures between R32 and R125 by using the experimental data from the works of Okada et al.[48]

and of Fröba and Leipertz[49] and mixtures between R125 and R152a by using the experimental data from the work of Bi et al.[50]. It is worth noticing that for these two types of mixture, there are data with only three different concentrations, so the temperature-dependent coefficient $C(T)$ in Eq. (31) is omitted so that the total number of temperature-dependent coefficients determining the BIPc is always inferior than the number of different concentrations in the experimental data. Thus, for these two types of mixtures, Eq. (31) can be defined as Eq. (46).

$$l_{12}(T, w_1) = w_1(1 - w_1)(A(T) + B(T)(w_1 - w_2)) \quad (46)$$

Table 10: Values of Eq.(44)'s parameters l_a, l_b and l_c for the R32 (1) +R125 (2) binary system.

w_1	44.3%	49.6%	50%
l_a ($\times 10^{-10}$K^{-1})	1.000	1.000	1.000
l_b ($\times 10^{1}$)	-2.345	-2.445	-4.329
l_c ($\times 10^{2}$K)	3.512	3.500	3.868
ARD (%)	4.6	4.6	4.4
BIAS (%)	-0.31	-0.36	-0.24

Table 11: Values of Eq.(44)'s parameters l_a, l_b and l_c for the R125 (1) +R152a (2) binary system.

w_1	9.7%	20.19%	29.96%
l_a ($\times 10^{-9}$K^{-1})	1.506($\times 10^{-3}K^{-1}$)	8.175	8.175
l_b ($\times 10^{1}$)	6.093	12.81	3.155
l_c ($\times 10^{2}$K)	4.369	7.377	3.840
AAD (%)	16	8.0	5.8
BIAS (%)	75	-6.4	-4.3

Table 12: Values of Eq. (31)'s parameters A and B for the R32+R125 binary system.

T /K	*A*	*B*	ARD /%	BIAS /%
240	1.006	1.385	9.2	1.2
250	1.097	1.447	8.4	1.0
260	1.207	1.502	7.5	0.79
270	1.339	1.5364	6.3	0.56
280	1.503	1.527	4.9	0.33
290	1.711	1.418	3.0	0.13
300	1.980	1.087	0.58	0.0048
310	2.339	0.2193	2.8	0.11
320	2.883	-2.098	7.5	0.80
330	3.519	-9.148	14	3.1
340	4.383	-38.43	24	10

Table 13: Values of Eq. (31)'s parameters A and B for the R125+R152a binary system.

T /K	*A*	*B*	AAD /%	BIAS /%
240	-3.101	-4.486	8.3	21
250	-3.292	-4.713	8.3	19
260	-3.494	-4.932	8.3	17
270	-3.706	-5.136	8.1	15
280	-3.926	-5.313	7.8	13
290	-4.149	-5.447	7.3	9.9
300	-4.377	-5.523	6.6	6.8
310	-4.571	-5.479	5.4	3.9
320	-4.735	-5.305	3.6	1.4
330	-4.844	-4.965	0.87	0.060

The adjusted results for these two types of mixtures are shown in the following part. The first step for the adjustment of these two mixtures also consists of the reconstruction of the experiment data in order to obtain data under the same temperatures. Tables 10 and 11 show the corresponding adjusted parameters of the two mixtures. Then, these reconstructed data are used to calibrate the temperature-dependent coefficients A and B (Eq. (31)), the adjusted results are shown in Tables 12 and 13.

Similarly, since the third temperature dependent coefficient is omitted, only the first two equations concerning $A(T)$ and $B(T)$ in the Eq. (32) are used for the adjustment of these two temperature dependent coefficients. The adjusted results of the temperature-independent constants determining $A(T)$ and $B(T)$ for the two types of the mixtures are shown in Tables 14 and 15. Their ARD and BIAS are shown in Tables 16 and 17. Figs S3 and S4 present a comparison between the $A(T)$ and $B(T)$ calculated from the experimental data and from the estimated group of these temperature-independent constants.

With all these coefficients and constants adjusted for the two types of mixture, new predictions of the surface tension can also be acquired. The results of the predictions, compared with the original experimental data and with calculated surface tensions with unadjusted BIPc ($l_{12} = 0$) are shown in Fig. S5 and Fig. 4, while the ARDs for all the studied w_1 for the two types of mixtures are presented in Tables 18 and 19.

Table 14: Values of Eq. (32)'s temperature-independent parameters for the BIPc for the R32+R125 binary system.

Constant	Value	Constant	Value
$\boldsymbol{A_1}$ $(\times \mathbf{10^{-3}})$	2.330	$\boldsymbol{B_1}$ $(\times \mathbf{10^{-2}})$	1.173
$\boldsymbol{A_2}$ $(\times \mathbf{10^{2}})$	-2.219	$\boldsymbol{B_2}$ $(\times \mathbf{10^{2}})$	1.116
$\boldsymbol{A_3}$ $(\times \mathbf{10^{2}})$	3.825	$\boldsymbol{B_3}$ $(\times \mathbf{10^{2}})$	3.425

Table 15: Values of Eq. (32)'s temperature-independent parameters for the BIPc for R125+R152a binary system.

Constant	Value	Constant	Value
A_1 $(\times 10^{-3})$	-8.095	B_1 $(\times 10^{-2})$	-2.021
A_2 $(\times 10^{2})$	2.448	B_2 $(\times 10^{1})$	-2.799
A_3 $(\times 10^{2})$	4.342	B_3 $(\times 10^{2})$	3.462

Table 16: ARD and BIAS of values of fitting for *A* and *B* for the R32+R125 binary system.

	A	*B*
ARD /%	0.67	18
BIAS /%	-0.0067	-5.0

Table 17: ARD and BIAS of values of fitting for *A* and *B* parameters for R125+R152a binary system.

	A	*B*
ARD /%	1.9	1.1
BIAS /%	-0.062	-0.016

Table 18: ARD and BIAS for the predictions with adjusted BIPc compared to the experimental data for the three studied w_1 for R32 (1) +R125 (2) binary system.

w_1	44.3%	49.6%	50%
ARD /%	0.45	0.84	0.73
BIAS /%	-0.058	-0.068	0.62

Table 19: ARD and BIAS for the predictions with adjusted BIPc compared to the experimental data for the three studied w_1 for R125 (1) +R152a (2) binary system.

w_1	9.7%	20.19%	29.96%
ARD /%	0.88	1.9	0.84
BIAS /%	0.65	-1.8	0.48

As it can be seen from the figures and ARD, the adjustment implemented for the mixtures R32+R125 has a similar performance as that for the mixture R32+R134a: the prediction results with adjusted BIPc show great consistency with the experimental result, while they are much

closer than the prediction results with unadjusted BIPc (with $l_{12} = 0$). In addition, for the mixture R125+R152a, although the prediction results with the adjusted BIPc show also a great consistency with the experimental result, it's rather difficult to judge directly which one between the adjusted result and unadjusted result is better from the figures (especially Figs. 4 (a) and 4(b)). The ARD and the BIAS of the prediction with unadjusted BIPc are also calculated and shown in Table 20. By comparing these two values with those calculated with the adjusted BIPc, we can still observe that the predictions with the adjusted results are better since they have smaller ARD and the smaller absolute value of BIAS for all the studied concentrations.

In the end, it is worth mentioning that, due to a lack of experimental data, all the adjustments done in this work are done in the subcritical conditions, while the methods and correlations are valid for subcritical conditions. It is possible that different correlations can be found to better represent the situation under supercritical conditions with more experimental data in these conditions.

Table 20: ARD and BIAS for the predictions with unadjusted BIPc ($l_{12} = 0$) compared to the experimental data for the three studied w_1 for R32 (1) +R152a (2) binary system.

w_1	44.3%	49.6%	50%
ARD /%	0.93	3.3	5.3
BIAS /%	0.72	-3.3	-5.3

These results above have once again demonstrated both the necessity and effectiveness of the adjustment and prediction method proposed in this work.

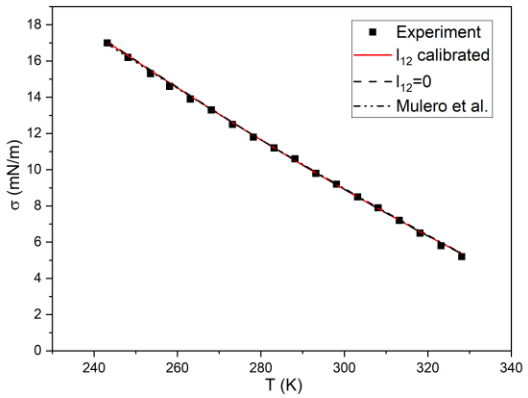

(a) w_1=9.7%

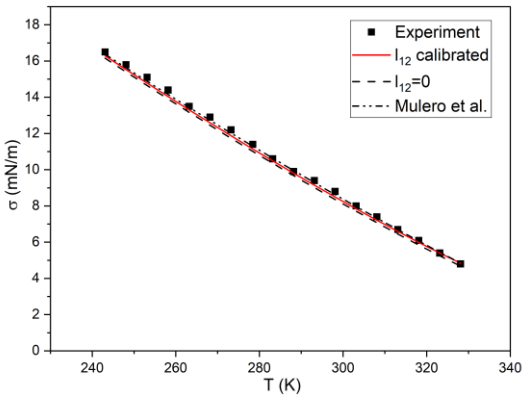

(b) w_1=20.19%

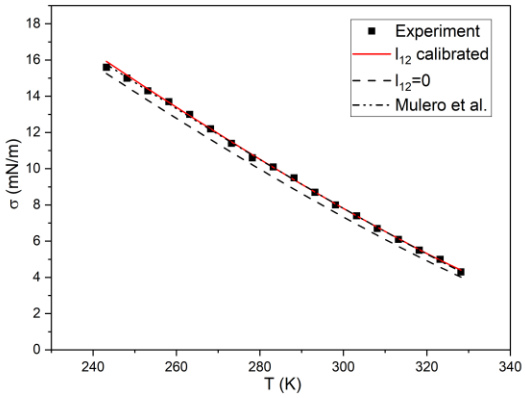

(c) w_1=29.96%

Figure 4: Surface tensions predicted by the model with the adjusted l_{12} compared with experimental data, with surface tensions calculated with unadjusted l_{12} ($l_{12} = 0$) and with method proposed by Mulero et al. (supplementary file) for mixture R125 (1) +R152a (2) binary system.

3.3.3 R32+R1234yf and R32+R1234ze(E)

Two systems with R32 (R32+R1234yf and R32+R1234ze(E)) are then studied by using the experimental data from Cui et al.[39]. This time, similar correlation of the l_{12} with only two temperature dependent coefficients is used since only data with three different group of concentrations are available in the literature for either of these mixtures. In the contrary, the molar fraction of component 1, x_1, is used in the correlation, instead of the mass fraction, w_1, since the data are based on the molar fraction. Thus, the Eq. (47) is used for these two mixtures.

$$l_{12}(T, x_1) = x_1(1 - x_1)(A(T) + B(T)(x_1 - x_2)) \quad (47)$$

The results of the adjustment of these two mixtures are shown in the Tables 21 to 24 for the R32+R1234yf binary system and in the Tables 25 to 28.

Table 21: Adjusted results of l_a, l_b and l_c for the R32 (1) +R1234yf (2) binary system.

x_1	51.93%	69.88%	79.45%
l_a ($\times 10^{-10}$K^{-1})	1.000	1.000	1.000
l_b ($\times 10^{1}$)	-1.911	-6.823	-6.051
l_c ($\times 10^{2}$K)	3.682	3.479	3.468
ARD (%)	4.9	24	26
BIAS (%)	-0.41	-11	-9.5

Table 22: Adjusted results of A and B for the R32+R1234yf binary system.

T /K	A	B ($\times 10^{-1}$)	AAD /%	BIAS /%
240	0.5226	-3.948	1.5	3.2
250	0.5697	-4.223	1.6	3.1
260	0.6261	-4.530	1.7	2.9
270	0.6946	-4.870	1.9	2.8
280	0.7797	-5.234	2.0	2.6
290	0.8880	-5.597	2.2	2.3
300	1.030	-5.878	2.4	2.0
310	1.224	-5.824	2.6	1.6
320	1.502	-4.565	2.8	1.1
330	1.920	1.771	2.8	0.58
343	2.584	110.2	5.5	0.19

Table 23: Adjusted results of the temperature-independent constants for the R32+R1234yf binary system.

Constant	Value	Constant	Value
A_1 ($\times 10^{-3}$)	-1.130	B_1 ($\times 10^{-3}$)	-2.663
A_2 ($\times 10^{2}$)	-1.098	B_2 ($\times 10^{1}$)	-1.465
A_3 ($\times 10^{2}$)	3.794	B_3 ($\times 10^{2}$)	-3.442

Table 24: ARD and BIAS of values of fitting for A and B parameters for the R32+R1234yf binary system.

	A	B
ARD /%	1.2	18
BIAS /%	-0.022	-4.7

Table 25: Adjusted results of l_a, l_b and l_c for the R32 (1) +R1234ze(E) (2) binary system.

x_1	29.85%	56.97%	75.01%
l_a ($\times 10^{-4}$K^{-1})	-4.580	-1.169	-3.804
l_b ($\times 10^{0}$)	-4.015	-3.933	-8.603
l_c ($\times 10^{2}$K)	3.556	3.544	3.573
ARD (%)	1.7	23	5.8
BIAS (%)	-1.1	-6.7	-6.4

Table 26: Adjusted results of *A* and *B* for the R32+R1234ze(E) binary system.

T /K	*A* ($\times 10^{-2}$)	*B* ($\times 10^{-1}$)	AAD /%	BIAS /%
295	0.5768	3.634	2.2	26
300	1.052	5.000	1.9	17
305	2.845	6.202	1.5	9.3
310	6.180	7.169	1.1	4.3
315	11.23	7.910	0.74	1.3
320	18.28	8.492	0.29	0.13
325	27.94	9.012	0.30	0.10
330	41.48	9.597	1.1	0.74
335	61.70	10.44	2.3	1.7
340	95.19	11.93	4.02	2.5
348	247.7	19.71	8.6	2.1

Table 27: Adjusted results of the temperature-independent constants for the R32+R1234ze(E) binary system.

Constant	Value	Constant	Value
A_1 ($\times 10^{-4}$)	-5.767	B_1 ($\times 10^{-2}$)	-1.523
A_2 ($\times 10^{2}$)	-9.778	B_2 ($\times 10^{2}$)	-8.321
A_3 ($\times 10^{2}$)	3.513	B_3 ($\times 10^{2}$)	4.671

Table 28: ARD and BIAS of values of fitting for *A* and *B* parameters for the R32+R1234ze(E) binary system.

	A	*B*
ARD /%	30	13
BIAS /%	-11	-2.4

In the end, the prediction results of the surface tensions for the two mixtures after adjustments, alongside with the comparison with the experimental data are shown in the following Tables 29 and 30, and Fig.S6 for the R32+R1234yf binary system and Fig.5 for R32 + R1234ze(E) binary

system.

Table 29: ARD and BIAS for the predictions with adjusted BIPc compared to the experimental data for the three studied x_1 for the R32 (1) +R1234yf (2) binary system.

x_1	51.93%	69.88%	79.45%
ARD /%	1.0	6.8	4.7
BIAS /%	0.79	-2.6	0.66

Table 30: ARD and BIAS for the predictions with adjusted BIPc compared to the experimental data for the three studied x_1 for the R32 (1) +R1234ze(E) (2) binary system.

x_1	29.85%	56.97%	75.01%
ARD /%	1.1	2.1	1.4
BIAS /%	-0.053	-0.15	1.3

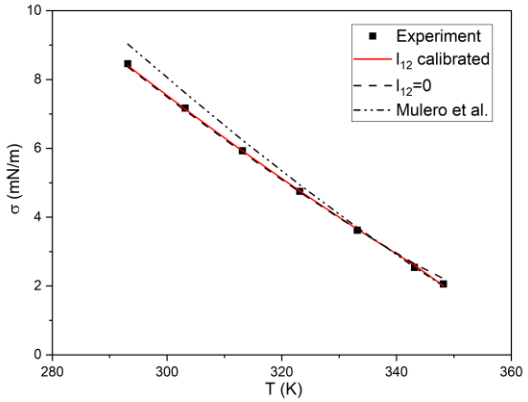

(a) x_1=29.85%

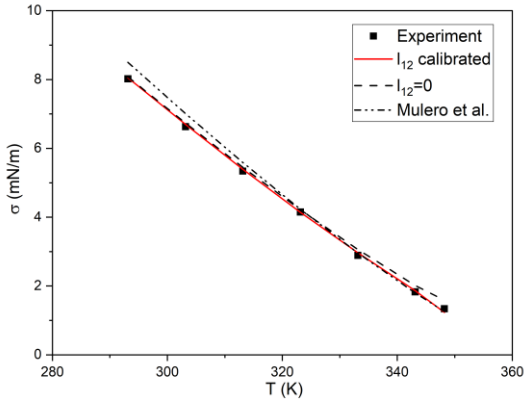

(b) x_1=56.97%

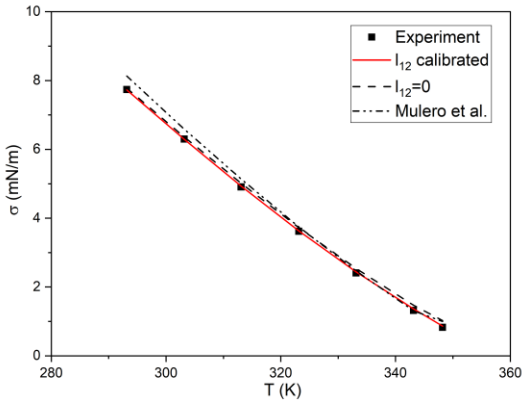

(c) x_1=75.01%

Figure 5: Surface tensions predicted by the model with the adjusted l_{12} compared with experimental data, with surface tensions calculated with unadjusted l_{12} ($l_{12} = 0$) and with method proposed by Mulero et al.

(supplementary file) for the R32 (1) +R1234ze(E) (2) binary system.

3.3.4 R143a+R134a binary system

In the end, the binary system between R143a and R134a is also studied under three different compositions (thus, eq.(47) is used for the BIPc), by using the experimental data of Lin and Duan [51]. The detailed results are shown in the supplementary file.

4 Remarks and Conclusion

In this work, based on the Linear Gradient Theory, a novel model combining the Peng-Robinson Equation of State has been proposed. In this model, we have also proposed correlations representing the PSIP and the BIP for the influence parameter, alongside the methods to calibrate and obtain the expression for these two parameters. These improvements have greatly optimized the model. With the proposed model, the surface tensions of several common pure refrigerants are calculated while their PSIP is adjusted. By using these adjusted parameters, and with the help of the experimental data in the prior works, the BIPcs of several binary mixture of are adjusted for the subcritical scenario. The calculation result with the adjusted BIPc shows a great consistency with the experimental data, and a great improvement compared to the result obtained with the unadjusted BIPc.

With our approach, we can observe that the BIP for the influence parameter *c* is temperature dependent as expected but also composition dependent. For a given temperature, the variation of the BIP with the composition is similar to a variation of a thermodynamic excess property. Far from the critical temperature, its value seems not to vary too much in the whole range of composition (not in infinite dilution region). As we have selected an equation of state not so accurate in liquid density prediction, particularly close to the critical point, it could be interesting to observe if we have similar behavior with an equation of state more accurate for density prediction.

References

1. Lin, H. and Y. Duan, *Surface Tension of 1, 1, 1-Trifluoroethane (HFC-143a), 1, 1, 1, 2, 3, 3, 3-Heptafluoropropane (HFC-227ea), and Their Binary Mixture HFC-143a/227ea.* International Journal of Thermophysics, 2003. **24**(6): p. 1495-1508.
2. Zhao, G., et al., *Surface tension of propane (R-290)+ 1, 1-Difluoroethane (R-152a)*

from (248 to 328) K. Journal of Chemical & Engineering Data, 2010. **55**(9): p. 3077-3079.

3. Macleod, D., *On a relation between surface tension and density.* Transactions of the Faraday Society, 1923. **19**(July): p. 38-41.

4. Sugden, S., *VI.—The variation of surface tension with temperature and some related functions.* Journal of the Chemical Society, Transactions, 1924. **125**: p. 32-41.

5. Sugden, S., *CXLI.—The influence of the orientation of surface molecules on the surface tension of pure liquids.* Journal of the Chemical Society, Transactions, 1924. **125**: p. 1167-1177.

6. Weinaug, C.F. and D.L. Katz, *Surface tensions of methane-propane mixtures.* Industrial & Engineering Chemistry, 1943. **35**(2): p. 239-246.

7. Guggenheim, E.A., *The principle of corresponding states.* The Journal of Chemical Physics, 1945. **13**(7): p. 253-261.

8. Kim, S.Y., S.S. Kim, and B. Lee, *Prediction of the surface tension of binary systems based on the partial least squares method.* Korean Journal of Chemical Engineering, 2009. **26**(2): p. 349-353.

9. Zuo, Y.X. and E.H. Stenby, *Corresponding-states and parachor models for the calculation of interfacial tensions.* The Canadian Journal of Chemical Engineering, 1997. **75**(6): p. 1130-1137.

10. Attard, P. and G.A. Moule, *A force-balance Monte Carlo simulation of the surface tension of a hard-sphere fluid.* Molecular Physics, 1993. **78**(4): p. 943-959.

11. Gloor, G.J., et al., *Test-area simulation method for the direct determination of the*

interfacial tension of systems with continuous or discontinuous potentials. The Journal of chemical physics, 2005. **123**(13): p. 134703.

12. Haile, J., C. Gray, and K. Gubbins, *Theory of surface tension for molecular liquids. II. Perturbation theory calculations.* The Journal of Chemical Physics, 1976. **64**(6): p. 2569-2578.

13. Toxvaerd, S., *Surface Structure of a Square-Well Fluid.* The Journal of Chemical Physics, 1972. **57**(10): p. 4092-4097.

14. Cahn, J.W. and J.E. Hilliard, *Free energy of a nonuniform system. I. Interfacial free energy.* The Journal of chemical physics, 1958. **28**(2): p. 258-267.

15. Miqueu, C., et al., *Modelling of the surface tension of pure components with the gradient theory of fluid interfaces: a simple and accurate expression for the influence parameters.* Fluid phase equilibria, 2003. **207**(1-2): p. 225-246.

16. Miqueu, C., et al., *Modelling of the surface tension of binary and ternary mixtures with the gradient theory of fluid interfaces.* Fluid phase equilibria, 2004. **218**(2): p. 189-203.

17. Rowlinson, J.S., *Translation of JD van der Waals'"The thermodynamik theory of capillarity under the hypothesis of a continuous variation of density".* Journal of Statistical Physics, 1979. **20**(2): p. 197-200.

18. Carey, B., L. Scriven, and H. Davis, *Semiempirical theory of surface tensions of pure normal alkanes and alcohols.* AIChE Journal, 1978. **24**(6): p. 1076-1080.

19. Garrido, J.M., et al., *Interfacial tensions of industrial fluids from a molecular-based square gradient theory.* AIChE Journal, 2016. **62**(5): p. 1781-1794.

20. Lin, H., Y.-Y. Duan, and Q. Min, *Gradient theory modeling of surface tension for pure*

fluids and binary mixtures. Fluid phase equilibria, 2007. **254**(1-2): p. 75-90.

21. Hosseini, S., M. Sadeghi, and T. Zarei, *A combined density gradient theory with equation of state model for the study of surface tension of refrigerant fluids.* Journal of Molecular Liquids, 2022. **352**: p. 118629.

22. Larsen, P.M., B. Maribo-Mogensen, and G.M. Kontogeorgis, *A collocation method for surface tension calculations with the density gradient theory.* Fluid Phase Equilibria, 2016. **408**: p. 170-179.

23. Yang, A.J., P.D. Fleming III, and J.H. Gibbs, *Molecular theory of surface tension.* The Journal of Chemical Physics, 1976. **64**(9): p. 3732-3747.

24. Zuo, Y.-X. and E.H. Stenby, *A linear gradient theory model for calculating interfacial tensions of mixtures.* Journal of Colloid and Interface Science, 1996. **182**(1): p. 126-132.

25. Peng, D.-Y. and D.B. Robinson, *A new two-constant equation of state.* Industrial & Engineering Chemistry Fundamentals, 1976. **15**(1): p. 59-64.

26. Chabab, S., P. Paricaud, and C. Coquelet, *Détermination des propriétés thermodynamiques des fluides-Fluides purs.* 2020.

27. Qian, J.-W., et al., *Fluid-phase-equilibrium prediction of fluorocompound-containing binary systems with the predictive E-PPR78 model.* International Journal of Refrigeration, 2017. **73**: p. 65-90.

28. Zuo, Y.-X. and E.H. Stenby, *Calculation of interfacial tensions with gradient theory.* Fluid phase equilibria, 1997. **132**(1-2): p. 139-158.

29. Schmidt, K.A., G.K. Folas, and B. Kvamme, *Calculation of the interfacial tension of*

the methane–water system with the linear gradient theory. Fluid Phase Equilibria, 2007. **261**(1-2): p. 230-237.

30. Carey, B.S., *THE GRADIENT THEORY OF FLUID INTERFACES*. 1979: University of Minnesota.

31. Mulero, A., I. Cachadiña, and M. Parra, *Recommended correlations for the surface tension of common fluids.* Journal of Physical and Chemical Reference Data, 2012. **41**(4): p. 043105.

32. Yufei, L., et al., *Surface Tension and Parachor for a New Low-GWP Refrigerant R1123/R32/R1234yf and its Constituent Binary Pairs.* International Journal of Refrigeration, 2021.

33. Heide, R., *The surface tension of HFC refrigerants and mixtures.* International journal of refrigeration, 1997. **20**(7): p. 496-503.

34. Kondou, C., et al., *Surface tension of low GWP refrigerants R1243zf, R1234ze (Z), and R1233zd (E).* International Journal of Refrigeration, 2015. **53**: p. 80-89.

35. Tanaka, K. and Y. Higashi, *Thermodynamic properties of HFO-1234yf (2, 3, 3, 3-tetrafluoropropene).* International journal of refrigeration, 2010. **33**(3): p. 474-479.

36. Zhao, G., et al., *Liquid viscosity and surface tension of R1234yf and R1234ze under saturation conditions by surface light scattering.* Journal of Chemical & Engineering Data, 2014. **59**(4): p. 1366-1371.

37. Zhao, X., et al., *Measurements of Surface Tension of R1234yf and R1234ze (E).* Journal of Chemical & Engineering Data, 2018. **63**(1): p. 21-26.

38. Tillner-Roth, R. and A. Yokozeki, *An international standard equation of state for*

difluoromethane (R-32) for temperatures from the triple point at 136.34 K to 435 K and pressures up to 70 MPa. Journal of Physical and Chemical Reference Data, 1997. **26**(6): p. 1273-1328.

39. Cui, J., et al., *Surface tension and liquid viscosity of R32+ R1234yf and R32+ R1234ze.* Journal of Chemical & Engineering Data, 2016. **61**(2): p. 950-957.

40. Lemmon, E.W. and R.T. Jacobsen, *A new functional form and new fitting techniques for equations of state with application to pentafluoroethane (HFC-125).* Journal of Physical and Chemical Reference Data, 2005. **34**(1): p. 69-108.

41. Outcalt, S.L. and M.O. McLinden, *A Modified Benedict–Webb–Rubin Equation of State for the Thermodynamic Properties of R152a (1, 1-difluoroethane).* Journal of Physical and Chemical Reference Data, 1996. **25**(2): p. 605-636.

42. Tillner-Roth, R. and H.D. Baehr, *An international standard formulation for the thermodynamic properties of 1, 1, 1, 2 - Tetrafluoroethane (HFC - 134a) for temperatures from 170 K to 455 K and pressures up to 70 MPa.* Journal of Physical and Chemical Reference Data, 1994. **23**(5): p. 657-729.

43. Lemmon, E.W. and R.T. Jacobsen, *An international standard formulation for the thermodynamic properties of 1, 1, 1-trifluoroethane (HFC-143a) for temperatures from 161 to 450 K and pressures to 50 MPa.* Journal of Physical and Chemical Reference Data, 2000. **29**(4): p. 521-552.

44. Akasaka, R. and E.W. Lemmon, *Fundamental equations of state for cis-1, 3, 3, 3-tetrafluoropropene [R-1234ze (Z)] and 3, 3, 3-trifluoropropene (R-1243zf).* Journal of Chemical & Engineering Data, 2019. **64**(11): p. 4679-4691.

45. Akasaka, R., *Recent trends in the development of Helmholtz energy equations of state and their application to 3, 3, 3-trifluoroprop-1-ene (R-1243zf).* Science and Technology for the Built Environment, 2016. **22**(8): p. 1136-1144.

46. Mulero, A. and I. Cachadiña, *Recommended correlations for the surface tension of several fluids included in the REFPROP program.* Journal of Physical and Chemical Reference Data, 2014. **43**(2): p. 023104.

47. Duan, Y.-Y., H. Lin, and Z.-W. Wang, *Surface tension measurements of difluoromethane (R-32) and the binary mixture difluoromethane (R-32)+ 1, 1, 1, 2-tetrafluoroethane (R-134a) from (253 to 333) K.* Journal of Chemical & Engineering Data, 2003. **48**(4): p. 1068-1072.

48. Okada, M., et al., *Surface tension of HFC refrigerant mixtures.* International journal of thermophysics, 1999. **20**(1): p. 119-127.

49. Fröba, A. and A. Leipertz, *Thermophysical properties of the refrigerant mixtures R410A and R407C from dynamic light scattering (DLS).* International journal of thermophysics, 2003. **24**(5): p. 1185-1206.

50. Bi, S., G. Zhao, and J. Wu, *Surface tension of pentafluoroethane+ 1, 1-difluoroethane from (243 to 328) K.* Fluid phase equilibria, 2009. **287**(1): p. 23-25.

51. Lin, H. and Y.Y. Duan, *Surface Tension for the 1,1,1-Trifluoroethane (R-143a) + 1,1,1,2-Tetrafluoroethane (R-134a) System.* Journal of Chemical & Engineering Data, 2004. **49**(2): p. 372-375.